

铝合金搅拌摩擦焊 – 交叉点焊工艺

周冠男¹, 沈以赴¹, 李 博¹, 姚 磊^{1*}, 胡伟叶²

(1. 南京航空航天大学 材料科学与技术学院, 南京 210016;

2. 中国航天科工集团 南京晨光厂工艺研究所, 南京 210012)

摘 要: 在铝合金传统搅拌摩擦点焊的基础上, 以提高点焊接头力学性能为目标, 提出“搅拌摩擦焊 – 交叉点焊”技术。其基本工艺原理是: 搅拌头沿交叉轨迹做极短距离的往复式搅拌摩擦焊, 以实现高性能的点焊连接。对 4 mm 板厚 5A02-H14 铝合金进行“搅拌摩擦焊 – 交叉点焊”试验及分析。结果表明, 该工艺可大大拓宽点焊接头的连接面积, 并显著降低搭接界面畸变和匙孔处材料缺失的不利影响, 与传统搅拌摩擦点焊相比, 该工艺能够显著提高铝合金点焊接头的抗剪切性能。

关键词: 交叉点焊; 搅拌摩擦焊; 铝合金; 力学性能

中图分类号: TG 453 **文献标识码:** A **文章编号:** 0253-360X(2014)05-0071-04

0 序 言

铝合金作为运载工具的主要制造材料已广泛应用于航空航天飞行器制造、汽车制造等行业中。近年来针对铝合金开发的点式连接技术有电阻焊、铆接、胶接及熔化焊等, 而随着搅拌摩擦点焊的问世及发展, 该技术对铝合金连接所特有的优势日益突显, 并逐渐替代传统的连接技术^[1]。搅拌摩擦点焊 (friction stir spot welding, FSSW) 是由先进的搅拌摩擦焊 (FSW) 技术衍生出来的, 其本身的技术特点可实现对复杂结构件的点式连接, 但在实际应用中, 铝合金 FSSW 技术也存在着一些不足, 如 FSSW 点焊接头强度相对较低, 无法达到某些结构件的力学指标要求。因此, 如何提高搅拌摩擦点焊接头力学性能是目前研究的重点问题。

目前, 提高 FSSW 接头力学性能通常采取的方法包括: (1) 优化传统 FSSW 的工艺参数, 但由于传统 FSSW 本身的弊端^[2]: 过小的接头连接面积、匙孔处材料的缺失、搭接界面畸变的不利影响都限制了其接头力学性能的提高; (2) 研发新的 FSSW 技术, 如无匙孔搅拌摩擦点焊^[3]等, 而现已开发的技术虽然一定程度上提高了 FSSW 的接头性能, 但其增加了设备研制的难度与成本的投入, 且令焊接过程更

为复杂, 大大增加技术的应用难度。文中在传统 FSSW 的基础上, 创新的提出“搅拌摩擦焊 – 交叉点焊” (cross-friction stir spot welding, cross-FSSW) 的技术方法, 并对其接头组织形貌进行了研究, 同时与传统 FSSW 的接头力学性能作了对比分析。

1 试验方法

试验选用母材为强度较高、耐腐蚀的 4 mm 厚 5A02-H14 铝合金板 (0.1Cu-0.4Si-0.1Mn-2.1Mg-0.1Zn-0.4Fe-0.15Ti, 质量分数, %) , 并依据国家标准 GB2649 制备点焊抗剪切试样用于力学性能测试, 其所制备试样如图 1 所示。试验中, 搅拌头材料为 H13 钢, 其硬度可达 45HRC 以上, 为保证数据具有可靠的对比性, cross-FSSW 和 FSSW 工艺试验均采用相同形貌的搅拌头: 搅拌针呈圆台形并带有螺纹, 轴肩直径为 24 mm, 针根部直径为 10 mm, 顶部直径为 8 mm, 针长为 7 mm。

根据前期优化试验选定 FSSW 的主要工艺参数: 旋转频率 $n = 1\ 400\ \text{r/min}$, 压入速度 $v = 2\ \text{mm/min}$, 停留时间 $t = 5\ \text{s}$, 压入量 $d = 0.2\ \text{mm}$ 。在 cross-FSSW 试验中也选用同样的参数, 但较传统 FSSW 的工艺参数加入了移动速度 (v_s)、移动距离 (L) 和移动下压量 (D) 三个参量。根据初步试验结果确定 L 值为 5 mm、 D 值为 0.05 mm, 并针对 v_s 值选取 4 组参数 (1, 5, 10, 20 mm/min) 进一步做工艺优化试验。焊后对接头试样进行金相腐蚀及光学显微观察, 选用腐蚀剂为 Keller 试剂, 并改变其配比

收稿日期: 2012-11-08

基金项目: 南京航空航天大学博士学位论文创新与创优基金资助项目 (BCXJ12-09); 中央高校基本科研业务费专项资金资助项目

* 参加此项研究工作的还有吴小伟

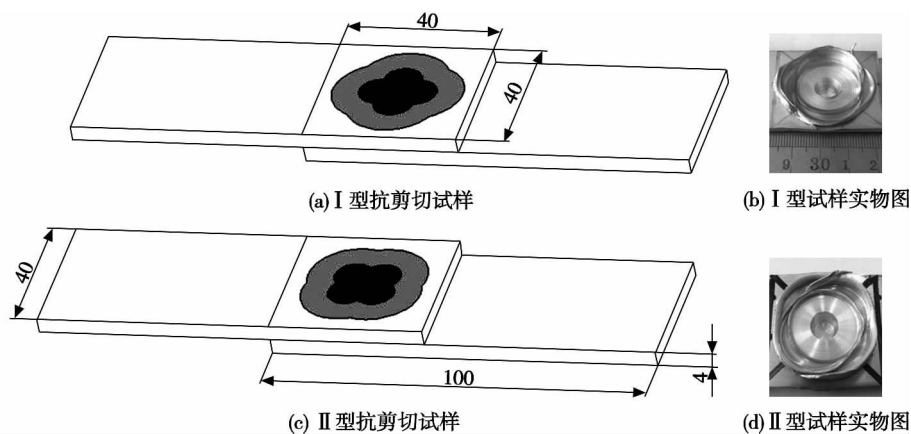


图 1 cross-FSSW 抗剪切试样及其典型接头宏观形貌示意图 (mm)

Fig. 1 Schematic illustration of lap-shear specimens and typical joints with cross-FSSW

(HF: HNO₃: H₂O = 2: 5: 190) .

在力学性能测试中, 因 cross-FSSW 接头特有的对称外形及为了便于研究, 仅制备两种典型的抗剪切试样如下.

I 型试样, 其受剪切力是沿搅拌头交叉往复行走的轨迹, 如图 1b 所示.

II 型试样, 其受剪切力方向与搅拌头交叉往复行走轨迹呈 45°, 如图 1d 所示.

采用 SANS 电子万能试验机在常温下进行测试, 拉伸速率为 1 mm/min.

2 技术原理及工艺参数选取

cross-FSSW 是基于搅拌摩擦点焊的改进技术, 其技术工艺原理是通过高速旋转的搅拌头在完全压入母材后, 并以压入点为原点, 沿交叉轨迹做极短距离的往复运动, 以实现高性能的点焊连接.

对于搅拌头的交叉往复移动需要通过数控编程, 在 xyz 三轴方向设定搅拌头行走轨迹路线, 共分为 6 个步骤, 移动示意图如图 2 所示. 需要说明的是, cross-FSSW 最终也会与传统 FSSW 一样仍会在焊后留下匙孔.

在对 cross-FSSW 特有的三个工艺参数 (v_s , D , L) 选取方面, 优先考虑 L 值的选取, 这是为避免多道焊对 cross-FSSW 接头组织的影响, 即抑制焊后组织出现过时效现象^[4], 必须使连接区域尽可能处于“一次焊”区域. 因此选取 L 值为搅拌针直径长度的 $1/2$ (5 mm), 使连接面积中“一次焊”区域最大, “四次焊”区域最小, 如图 3 所示.

对于选取 D 值, 即搅拌头在十字交叉移动中每一步的下压量, 通过前期初步试验发现: 如果 $D = 0$, 则会使 cross-FSSW 接头出现弱结合、孔洞等缺陷,

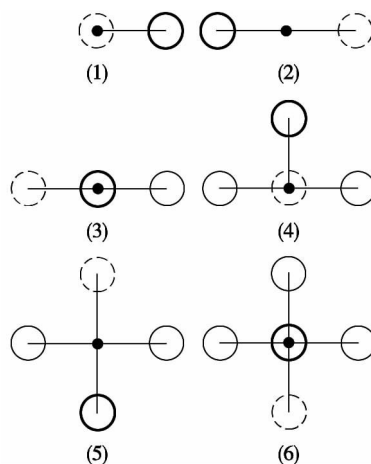


图 2 cross-FSSW 交叉往复移动示意图

Fig. 2 Schematic illustration of the cross-reciprocating motion principle of cross-FSSW

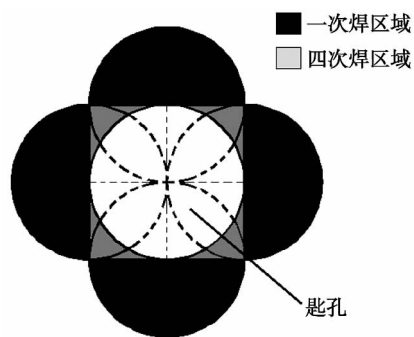


图 3 cross-FSSW 接头连接区域示意图

Fig. 3 Schematic illustration of welding areas of cross-FSSW joint

严重影响接头的力学性能; 而 D 值过大, 则会使上层母材板厚大大减小, 受力时会优先在上层板出现断裂, 同样会降低接头力学性能, 因此选取试验结果相对较好的 D 值为 0.05 mm. v_s 值为试验待测定

参数.

3 试验结果与讨论

3.1 cross-FSSW 接头组织特征

cross-FSSW 接头沿搅拌头交叉行走轨迹中心线所截试样的宏观形貌如图 4 所示,其组织与 FSSW 接头组织基本相似,同样存在焊核区 (SZ)、热力影响区 (TMAZ)、热影响区 (HAZ)、轴肩影响区 (SAZ)、母材区 (BZ). 在搭接界面处,上下母板的界面畸变(即 Hook 钩)的形貌也不在如传统 FSSW 一样弯曲向上至上层板^[5],而是向下翘曲,如图 4b 所示,这是由于 D 值的存在,使上下母材的迁移规律发生改变所致. 在搅拌头移动的过程中,随着 D 值的增加,上层板的大量塑化材料在轴肩的压力下急剧向下的迁移至下层板;同时由于焊接衬板的支撑作用,一部分下层板材料在弯曲、变形后,沿着搅拌针边缘被迁移至上层板,最终在界面处相遇,但与传统 FSSW 界面形貌不同的是其上下层板迁移材料不会发生激烈的碰撞,形成传统 FSSW 界面畸变中的典型的“锯齿”状形貌,而是随着搅拌头的移动交错开来,并迅速冷却、沉淀形成具有一定宽度的“耳廓”形区域,如图 4b 所示,此时界面畸变也变成弯曲向下的形貌.

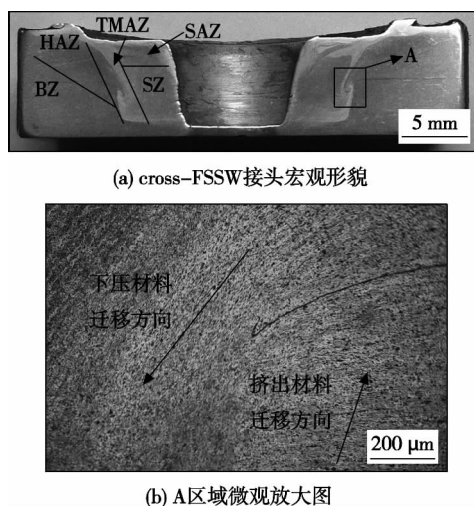


图 4 cross-FSSW 接头宏观截面形貌

Fig. 4 Cross-sectional macrographs of cross-FSSW joint

3.2 cross-FSSW 接头力学性能

通过对不同 v_s 值下的两种抗剪切试样进行力学性能测试,所得结果如表 1 所示.

测试结果表明: v_s 值的改变对于 cross-FSSW 接头的抗剪切力学性能没有显著的影响,在 $v_s = 10$

表 1 不同搅拌头交叉往复移动速度所得的接头力学性能
Table 1 Property of cross-FSSW joints with different v_s

搅拌头交叉往复移动速度 $v_s / (\text{mm} \cdot \text{min}^{-1})$	I 型试样断裂载荷 F_I / kN	II 型试样断裂载荷 F_{II} / kN
1	14.1	14.7
5	15.1	16.0
10	15.6	16.6
20	15.5	16.3

mm/min 时所得的接头抗剪切力学性能相对较好; I 型接头和 II 型接头的断裂载荷无太大差别,即剪切力的方向对 cross-FSSW 接头的抗剪切性能无太大影响.

对 $v_s = 10 \text{ mm/min}$ 的 I 型试样接头试样和 II 型接头试样断口进行观察,如图 5 所示. 分析发现:无论是 I 型接头试样还是 II 型接头试样, cross-FSSW 接头的断裂起始位置都在界面畸变的末端,而最终裂纹都不会在贯穿匙孔后使接头失效,失效形式属于上层板或下层板母材的断裂. 区别是 I 型接头的裂纹,由交叉接头的一处界面畸变形貌而演变生成,如图 5a 箭头所示,并沿界面畸变的翘曲方向扩展,最终使下层板完全断裂失效;而对于 II 型接头,因其对称的结构,裂纹产生位置会在两处界面畸变位置生成,如图 5b 箭头所示,并通过扩展生成一条长裂

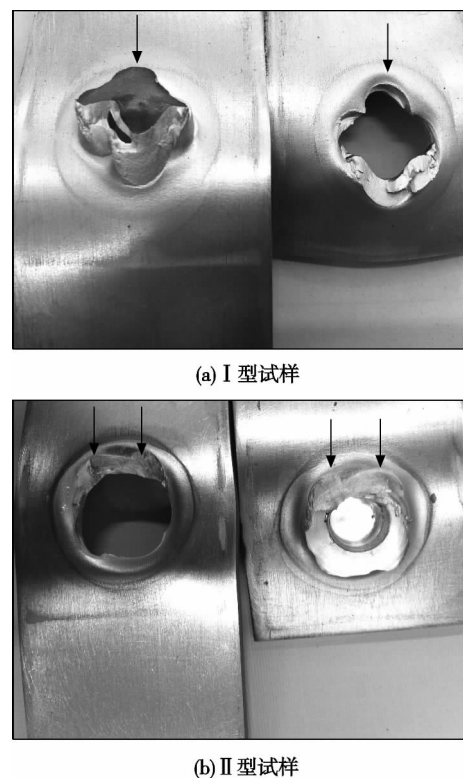


图 5 cross-FSSW 接头破坏形式

Fig. 5 Fracture modes of cross-FSSW joints

纹,使裂纹扩展的阻力增大,且由于上层板略薄于下层板,断裂路径更易于沿减薄的上层板扩展,最终使上层板断裂失效。

同时对在最佳参数下所得的 FSSW 接头和 cross-FSSW 两种接头试样进行抗剪切性能测试,并绘制对应的力—位移曲线,如图 6 所示。可以看出传统 FSSW 的断裂载荷为 7.3 kN,而 I 型接头和 II 型接头的断裂载荷分别是 15.6、16.6 kN,均约为传统 FSSW 的断裂载荷的 2 倍,因此无论是 I 型接头,还是 II 型接头,其抗剪切性能都远远优于传统 FSSW 接头。此外, cross-FSSW 接头的断后伸长率同样远大于传统 FSSW 接头,其中 I 型接头的断后伸长率相对较高,约为传统 FSSW 接头 7 倍左右。

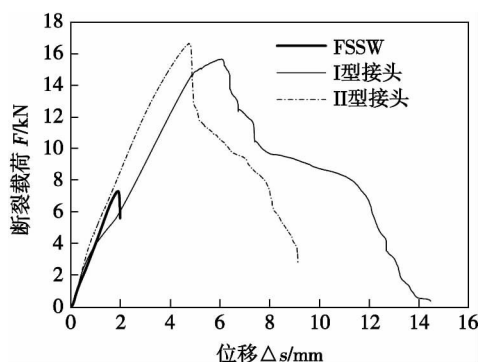


图 6 FSSW 和 I 型及 II 型接头试样的力—位移曲线

Fig. 6 Force-displacement curves of FSSW joint, sample I and sample II

4 结 论

(1) 基于提升搅拌摩擦点焊接头力学性能为目的,提出“搅拌摩擦焊—交叉点焊”的新型技术,该技术可以增加接头的有效连接面积,并最大程度上克服界面畸变和匙孔处材料缺失的影响。

(2) cross-FSSW 的接头组织基本与传统 FSSW

接头组织相同,但其焊核区宽度远大于传统搅拌摩擦点焊,且接头界面畸变形貌与传统搅拌摩擦点焊畸变形貌完全不同,其界面畸变末端向下层板方向弯曲,且畸变角度相对较小。

(3) cross-FSSW 接头质量明显优于传统 FSSW 接头,且受剪切力的方向对接头抗剪切力学性能无显著影响,接头的断裂载荷约为传统 FSSW 接头的 2 倍,其断后伸长率约为传统 FSSW 接头的 7 倍。

参考文献:

- [1] 张 华,林三宝,吴 林,等. 搅拌摩擦焊研究进展及前景展望[J]. 焊接学报,2003,24(3): 91-96.
Zhang Hua, Lin Sanbao, Wu Lin, et al. Current progress and prospect of friction stir welding [J]. Transactions of the China Welding Institution, 2003, 24(3): 91-96.
- [2] 尹玉环,胡绳荪,张晓博,等. AZ31 镁合金搅拌摩擦点焊[J]. 焊接学报,2011,32(3): 101-104.
Yin Yuhuan, Hu Shengsun, Zhang Xiaobo, et al. Friction stir spot welding of AZ31 Mg-alloy [J]. Transactions of the China Welding Institution, 2011, 32(3): 101-104.
- [3] 严 铿,方 圆. 工艺参数对填充式搅拌摩擦无匙孔点焊性能的影响[J]. 焊接学报,2010,31(10): 93-96.
Yan Keng, Fang Yuan. Influence of processing parameters on performance of friction stir spot welding with re-filling probe hole [J]. Transactions of the China Welding Institution, 2010, 31(10): 93-96.
- [4] Robson J, Upadhyay P, Reynolds A. Modelling microstructural evolution during multiple pass friction stir welding [J]. Science and Technology of Welding & Joining, 2010, 15(7): 613-620.
- [5] Badarinarayan H, Yang Q, Zhu S. Effect of tool geometry on static strength of friction stir spot-welded aluminum alloy [J]. International Journal of Machine Tools and Manufacture, 2009, 49(2): 142-149.

作者简介: 周冠男,男,1987 年出生,硕士研究生。主要从事搅拌摩擦点焊工艺研究。Email: zgn1987@sohu.com

通讯作者: 沈以赴,男,教授,博士研究生导师。Email: yifushen_nuaa@hotmail.com

mula. The result shows that although the repair welding degrade the welding joint property to some extent , it is still an efficient method to make sure the structure with flaw has enough load-carrying capacity.

Key words: aluminium alloy; repair welding; fatigue life

Numerical simulation on fracture parameter J-integral for narrow gap welding

TAN Long¹ , ZHANG Jianxun¹ , ZHANG Congping² (1. State key laboratory for mechanical behavior of materials , Xi'an Jiaotong University , Xi'an 710049 , China; 2. Dongfang steam turbine limited company , Deyang 618000 , China) . pp 55 – 58

Abstract: The microshear test has been developed to investigate the microshear strength of AP1000 Nuclear Steam Turbines rotor and its narrow gap welded joints. According to the relationship between shear strength and yield strength of metal , yield strength of the whole welding joints could be obtained. The influence of welding joint property nonuniformity on the J-integral was investigated by using finite element method. The simulated results indicated that the increase of the load may get rise in the value of J-integral. When the load increases to 0.8 times the limit load , crack tip enters into plastic area and the value of J-integral increases rapidly. For the same crack length and load , the J-integral value of under-matched area is higher than the one of the over-matched area , but the property nonuniformity of matching in loading area will cause the fluctuation of J-integral value.

Key words: welded joint; micro-region performance; finite element; fracture parameter

High temperature brazing of Si₃N₄ ceramic using Cu-Ti active filler metal

ZHANG Deku¹ , ZHANG Wenjun^{1,2} , JIANG Jiamin¹ (1. School of Materials Science and Engineering , Nanjing University of Science and Technology , Nanjing 210094 , China; 2. Luoyang Sunrui Special Alloy materials Co. , Ltd. , Luoyang 471039 , China) . pp 59 – 62

Abstract: Self-joining of Si₃N₄ using Cu80Ti20 active filler metal was demonstrated under different process parameters. Joints with no defects and cracks were obtained as the holding time is about 5-15 min and brazing temperature is about 1 413–1 493 K. The results shown that the microstructure of the joint can be described as Si₃N₄ ceramic/TiN layer/Cu-Ti solid solution + Ti₅Si₃/TiN layer/Si₃N₄ ceramic. On the condition of 1 413 K/10 min , Element Ti of solid solution diffused to the interface and reacted with ceramic , then compact and continuous reaction layer of thickness about 1 μm formed. The effects of brazing temperature and holding time on the width of the brazing seam , interface layer and the strength of joint were investigated , respectively. On the prescribed experiment condition shear strength of joint was up to 105 MPa.

Key words: silicon nitride ceramic; active filler metal; high temperature brazing; Cu-Ti

Effects of surface qualities on corrosion performances of X80 pipeline steel welded joints by laser shock processing

KONG Dejun¹ , YE Cundong¹ , WANG Wenchang² , FANG Xiaodong³ (1. College of Mechanical Engineering , Changzhou Uni-

versity , Changzhou 213016 , China; 2. School of Petrochemical Engineering , Changzhou University , Changzhou 213164 , China; 3. Jiangsu Provincial (Tongyu) Weld Pipe Engineering Research Center , Yangzhou 225008 , China) . pp 63 – 66

Abstract: The surface of X80 steel pipeline welded joint was processed with laser shock processing (LSP) , and the microstructure and roughness of welded joint before and after LSP was analyzed with metallographic microscope and optical profilometer , respectively. The changes of residual stress and residual austenite of welded joint before and after LSP were measured with stress tester , the mechanism of improving the surface qualities of welded joint by LSP was also discussed. The results show that the grain refinement of X80 pipeline steel welded joint is produced by LSP , the surface roughness has increased a little. The compressive residual stress is formed by LSP , and residual austenite is transformed into martensite. The effect of surface roughness and residual austenite by LSP on its tension performances is a main factor , its inner product power decreases 3.8% . The sensitivity index ISCC of stress corrosion of the sample by LSP decreases from 50.94% to 45.10% , the compressive residual stress and refined grain are the main mechanisms of affecting its stress corrosion resistance.

Key words: laser shock wave; welded joint of X80 pipeline steel; surface roughness; residual stress; residual austenite

Corrosion fatigue performance of 2205 DSS welded joints

WANG Zhixiang^{1,2} , ZHANG Yao² , ZHANG Jixiang² (1. Marine Engineering Center , Chongqing Jiaotong University , Chongqing 400074 , China; 2. Electromechanical and Automotive Engineering School , Chongqing Jiaotong University , Chongqing 400074 , China) . pp 67 – 70

Abstract: The corrosion fatigue performance of welded joints of homemade 2205 duplex stainless steel (DSS) has been studied in simulated seawater environment. The S – N curves of corrosion fatigue life were obtained at different environment temperatures of 24 , 30 and 40 °C , as the stress ratio is 0.1 and the loading frequency is 20 Hz. The experimental data shows that the low stress level had a significant effect on the fatigue life as environment temperature rising. Then an S – N mathematical model with temperature was established and welded joint fatigue limit was obtained in simulated seawater environment

Key words: 2205 duplex stainless steel; corrosion fatigue; S – N curve

A cross-friction stir spot welding process of aluminum alloy

ZHOU Guannan¹ , SHEN Yifu¹ , LI Bo¹ , YAO Lei¹ , WU Xiaowei¹ , HU Weiye² (1. College of Materials Science and Technology , Nanjing University of Aeronautics and Astronautics , Nanjing 210016 , China; 2. Technology Research Institute of Nanjing Chenguang Group Co. , Ltd (NCGC) , China Aerospace Science and Industry Corporation (CASTC) , Nanjing 210006 , China) . pp 71 – 74

Abstract: A new technique of cross-friction stir spot welding (cross-FSSW) was proposed for improving the mechanical properties of the spot weld joints. This technology was realized by the tool made the short cross-reciprocating movement. U-

sing this technique , experiments were conducted in 4 mm thick sheets of aluminum alloy 5A02 in H14 condition. The results show that the bonding widths of cross-FSSW joints had been increased , the adverse effects of interface distortion and the lack of material of the keyhole had been avoided. cross-FSSW joints were found to be superior to traditional Friction stir spot welds produced under optimum conditions in lap-shear.

Key words: cross-friction stir spot welding; friction stir welding; aluminum alloy; mechanical properties

The theory and application of the virtual fatigue test of welded structures based on the master S – N curve method

ZHAO Wenzhong¹ , WEI Hongliang^{1,2} , FANG Ji¹ , LI Jitao¹ (1. School of Traffic and Transportation Engineering , Dalian Jiaotong University , Dalian 116028 , China; 2. Technical Center of Qiqihar Rail Traffic Equipment Co , Qiqihar 161002 , China) . pp 75 – 78

Abstract: The necessity and feasibility of the virtual fatigue test technology of welded structure were discussed firstly. Then a basic theory of a new method called the master S – N curve method , which can be used for assessment of fatigue life of welded structure and published by the ASME (2007) standard , has been discussed as well. Following this discussion , a conclusion has been given that is the new method is resulted from the welded structure fatigue failure mechanism instead of fatigue failure test data. So this method is more suitable as the core algorithm in welding virtual fatigue test than nominal stress method. Finally , two applications have been given , and the results show that during the design phase , the welded structure virtual fatigue test technology based on the master S – N curve method , can effectively identify stress concentrations happened at each weld in a complex welding structure. In fact , this just is needed in design process.

Key words: welded structure; fatigue damage; virtual fatigue test; the master S – N curve; stress concentration

Laser welding technology of multi-chip subsystem shell and cover

YU Shenglin^{1,2} , XUE Songbai¹ , YAN Wei³ , JI Xu-an² , ZHU Xiaojun³ (1. College of Materials Science and Technology , Nanjing University of Aeronautics and Astronautics , Nanjing 210016 , China; 2. Nanjing University of Information Science and Technology , Nanjing 210044 , China; 3. Nanjing Research Institute of Electronics Technology , Nanjing 210039 , China) . pp 79 – 82

Abstract: Adopted the advantages of laser welding and by use of ANSYS software , the structure of the Al-50Si shell and the cover (4047 aluminum alloy) of the multi-chip subsystems which sealed by laser welding was analyzed , and the physical verification was also carried out. It was proved that structure form is the key factor which affected the quality of multi-chip subsystems which sealed by laser welding , the stress in laser weld of square structure is 36% higher than that in special-shaped structure (according to ANSYS analysis results) , and the air tightness of the square structure is lower by almost one order of magnitude than that of special-shaped structure , which performed by physical verification. The reason is that after laser welding , the welding

cracks induced by welding stress in the weld of square structure , so as to affect the air tightness of the weld. By adopt of special-shaped structure of multi-chip subsystems made from Al-50Si composite materials and the cover made from 4047 aluminum alloy , the stress in the welds can be effectively reduced , so the cracks in the weld are actually avoidable during laser welding. The result was indicated that the helium leak rate of the weld of special-shaped structure can reach to $8.9 \times 10^{-9} \text{ Pa} \cdot \text{m}^3/\text{s}$, which met the hermetic package requirement of multi-chip subsystems.

Key words: multi-chip; Al-Si alloys; laser welding; leakage rate

Virtual weld experiment system of billet flash butt welding process

LU Ning (School of Mechanical-Electronic and Automobile Engineering , Beijing University of Civil Engineering and Architecture , Beijing 100044 , China) . pp 83 – 87

Abstract: In view of the characteristics of flash welding system for large section rolling steel billet , mechanical kinematic models of welding equipments were built by using dynamics simulation software ADAMS. In which forging hydraulic servo system nonlinear model of the flash butt welding process was proposed in AMESim. Moreover , the servo control system for virtual welding system was built by utilizing the Simulink package of MATLAB software. By analysis of the data transmission characteristics between simulation softwares , a shared channel for dynamic data carrier was established by MATLAB software. A digital platform of welding electromechanical system was brought into forward , by which virtual experiment on electromechanical system of billet flash welding process can be carried out.

Key words: billet; flash butt weld; virtual experiment

Analysis of principle of least action on explosive welding process

SHI Changgen , ZHAO Linsheng , HOU Hongbao , WANG Yu (PLA University of Science Technology , Nanjing 210007 , China) . pp 88 – 90

Abstract: The principle of least action , basic law of the nature and the final rule of the physics , was found to be followed by the explosive welding process by theoretical analysis and interface test. Namely the optimal welding interface can be obtained with the least explosive charge. The bonding energy of the interface can be looked upon the action on the course. To minimize the bonding energy , these rules must be followed such as the lower limit of explosive charge , the upper limit of span and the explosive of the lower critical explosion velocity. The principle of least action is achieved on the explosive welding process , and the bonding interface will be best.

Key words: explosive welding; bonding interface; upper limit; lower limit

Investigation of thermal shock resistance of the nanostructured zirconia thermal barrier coatings treated by laser glazing

WANG Hongying , LI Zhijun , TANG Weijie , HAO Yunfei (Shenzhen Polytechnic , Shenzhen 518055 , China) . pp 91 – 94

Abstract: The nanostructured zirconia coatings were pre-